

Relativistic downshift frequency effects on ECE measurements of electron temperature and density in torus plasmas

M. Sato¹, A. Isayama¹, S. Inagaki², Y. Nagayama², K. Kawahata² and N. Iwama³

¹Japan Atomic Energy Research Institute, 801-1, Mukoyama, Naka, Ibaraki, 311-0193, Japan

²National Institute for Fusion Science, 322-6, Oroshi, Toki, Gifu, 509-5292, Japan

³Daido Institute of Technology, 10-3, Takiharu, Minami, Nagoya, 457-8530, Japan

Abstract

The measurement of electron density and temperature from electron cyclotron emission (ECE) is studied using a numerical calculation taking into account the relativistic effect. For the measurement of the electron temperature profile in Large Helical Device (LHD) in order to avoid the relativistic effect of 2nd harmonic ECE at the center and the absorption effect at the outer periphery, the location of the observing port should be at the opposite side of the highest magnetic field point with respect to the plasma center. The measurement of the electron density profile from ECE proposed can be applicable for various electron density profiles in tokamak.

1. Introduction

The importance of a relativistic frequency downshift effect on ECE in high temperature plasma is well recognized since the relativistic effects modify the relation between the frequency and the spatial position [1]. The relativistic downshift becomes very large at electron temperature (T_e) typically above 5 keV, and that the emissivity at the local position has a profile with finite extent in frequency. We present two results of numerical calculations about the relativistic effect on ECE. One is the relativistic effect on T_e profile measurement in LHD plasma, and the other is a feasibility of electron density (n_e) profile measurement from ECE in tokamaks.

2. Calculation methods

The emission and absorption processes in plasmas are described by the radiation transfer equation [2]. The emissivity is calculated using the formula obtained by Trubnikov for the case of perpendicular propagation relative to a magnetic field in a tenuous plasma [3]. The electron velocity-distribution function is assumed to be a spherically symmetric relativistic Maxwellian. The absorption coefficient is obtained from the emissivity applying Kirchhoff's law [2]. Since the refraction is neglected, the ray refractive index is taken as unity. The details of this

Table 1 Device parameters

Configuration	R_{axis} (m)	$2f_{ce}^0$ at R_{axis}
tokamak	3.4	223.9 GHz
LHD $\rho_{B_{\text{max}}}=0.2$	3.5	150.5 GHz
LHD $\rho_{B_{\text{max}}}=-0.18$	3.7	150.6 GHz

calculation method are given in ref. 1. The radial position of the T_e profile is determined by using the radial dependence of the non-relativistic 2nd harmonic electron cyclotron (EC) frequency ($2f_{ce}^0$). The major radius, R , and $2f_{ce}^0$ are shown in Table 1. The minor radius is 1m for tokamak.

3. Electron temperature profile measurement from ECE in LHD

Since the value of B_t has maximum along the sight line in LHD magnetic configuration, the emissivity at the maximum magnetic field is expected to decrease due to the relativistic effect. We have studied the relativistic effect in the cases that the position at maximum magnetic field locates at the magnetic axis [4,5]. Here we present the results at off-magnetic axis ($\rho_{B_{max}} = 0.2$ & -0.18), where $\rho_{B_{max}}$ is radial position at the maximum magnetic field. We consider only the observation from the outer side of torus for the calculation, that is, ECE is propagated from inner side of torus to outer side. The parametric dependences of the relativistic effect on T_e measurement was studied [5,6]. The T_e is higher and/or optical thickness is thinner, the deviation from the non-relativistic EC frequency is wider. Previous calculation showed that the T_e at the central region ($\Delta\rho < 0.2$) apparently decreases less than half even at 5 keV,

$n_e = 1 \times 10^{19} \text{ m}^{-3}$. The spatial variations of magnetic field are shown in Fig. 1 in the cases of off-magnetic axis configuration ($\rho_{B_{max}} = 0.2$ & -0.18), there is asymmetry of B_t aspect to the plasma axis, where f_i and f_o are the EC frequencies at the edge plasma of inner and outer side torus, respectively.

The ECE spectra in the case of parabolic electron temperature with $T_e(0) = 10 \text{ keV}$, and uniform electron density with $n_e = 1$ & $10 \times 10^{19} \text{ m}^{-3}$ are shown in Fig. 2. We found a slight change around $3f_o$ in the case of $n_e = 10 \times 10^{19} \text{ m}^{-3}$, $\rho_{B_{max}} = -0.18$, compared with the non-relativistic case. In the Fig.1 (b), the frequency of 2nd harmonic EC is overlapped at the frequency more than $3f_o$. When the n_e increases, the relativistic frequency downshift effect of 3rd harmonic EC at the outer periphery become dominant. The relativistic frequency down shifted 3rd harmonic ECE is emitted at the frequency more than $3f_o$, and the ECE is partially absorbed at the frequency less than $3f_o$. The peak at $f \sim 112 \text{ GHz}$ is caused by the outward

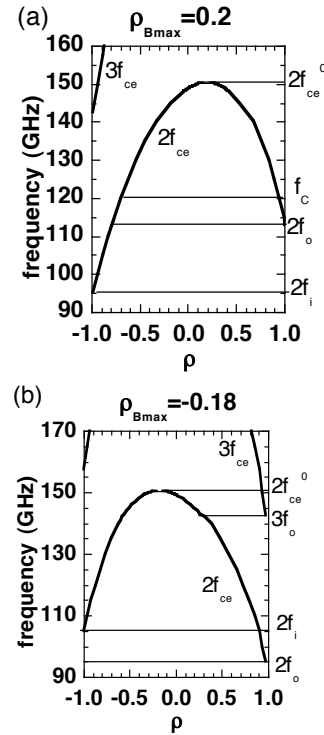


Fig.1. Spatial variation of magnetic field in the cases of (a) $\rho_{B_{max}} = 0.2$ and (b) -0.18

shifted magnetic configuration: ECE between $2f_i$ and $2f_o$ propagates in plasma without absorption in the case of $\rho_{B_{max}} = 0.2$. The combination of the asymmetry of B_r and absorption results in the peak near $2f_o$ in ECE spectra. In another configurations of LHD ($\rho_{B_{max}} = -0.18$), there is no peak in ECE spectra. Since $2f_i$ is bigger than $2f_o$, the ECE at the bigger frequency than $2f_i$ absorb at the outer periphery almost fully.

The T_e profiles obtained for the configurations of LHD in the case of $T_e(0) = 10$ keV, $n_e = 1$ & $10 \times 10^{19} \text{ m}^{-3}$ are shown in Fig. 3. The T_e profiles are normalized by the true value. There is apparent drop at the maximum of magnetic field. This is the relativistic effect of 2nd harmonic ECE at the non-relativistic EC frequency of the maximum B_r . In the case of $\rho_{B_{max}} = -0.18$, $n_e = 1 \times 10^{19} \text{ m}^{-3}$, the central T_e can be measured. On the other hand, in the case of $\rho_{B_{max}} = 0.2$, the central T_e can't be measured. We found the above-mentioned changes by 3rd relativistic effect for

$\rho_{B_{max}} = -0.18$, $n_e = 10 \times 10^{19} \text{ m}^{-3}$ and the increment due to the absorption effect for $\rho_{B_{max}} = 0.2$, $n_e = 10 \times 10^{19} \text{ m}^{-3}$. Since the T_e profile is slight shifted by the relativistic effect, the normalized temperature is slightly bigger than unity in the region $0.4 < \rho < 1.0$ in the cases of $\rho_{B_{max}} = -0.18$. When n_e increases, the shift decreases. These are the same behavior as the tokamak [6]

Here the relation between locations of the observing port (R_{ant}), the plasma center (R_{axis}), and the highest magnetic field ($R_{B_{max}}$) is discussed. Since calculation result in the case of outside observation is determined by the spatial location of magnetic configuration and magnetic axis, we can obtain the same results in the case of inside observation. So, in order to avoid the relativistic effect of 2nd harmonics and the absorption effect

at the outer periphery, The R_{ant} should be at the opposite side of $R_{B_{max}}$ with respect to R_{axis} i.e., $R_{ant} < R_{axis} < R_{B_{max}}$ or $R_{B_{max}} < R_{axis} < R_{ant}$ in LHD.

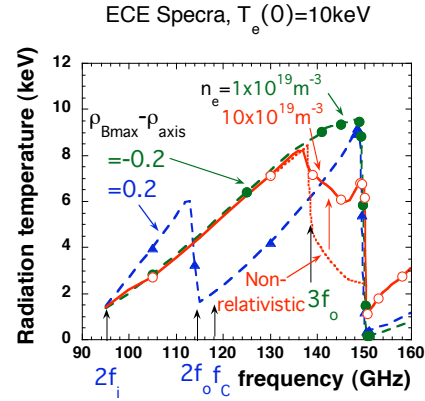


Fig.2. ECE spectra obtained in off-axis configurations ($\rho_{B_{max}} = 0.2$ (solid triangle: $n_e = 1 \times 10^{19} \text{ m}^{-3}$) and -0.18 (solid circle: $n_e = 1 \times 10^{19} \text{ m}^{-3}$; Open Circle: $n_e = 10 \times 10^{19} \text{ m}^{-3}$, broken line: non-relativistic case & $n_e = 10 \times 10^{19} \text{ m}^{-3}$).

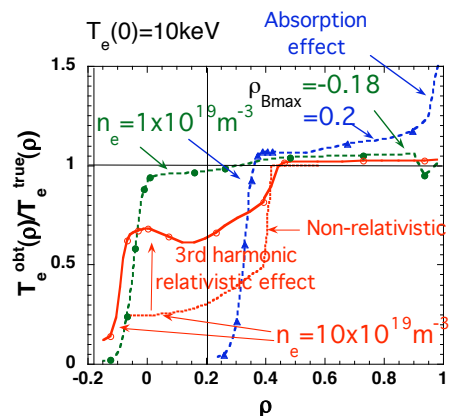


Fig.3. Normalized $T_e(\rho)$ obtained in the case of 10 keV,

4. Electron density measurement from ECE in tokamak

The relativistic effect results in the frequency shift from non-relativistic EC frequency. In a tokamak, the frequency shift due to the relativistic effect is observed from the high-field-side effectively. Since the shift depends on n_e , as well as T_e and B_r , there is a possibility of the n_e measurement by observing from both low- and high-field sides, and a feasibility of the n_e measurement has been confirmed by computational analysis [5, 7].

The mechanism for these relativistic effects on measurements is given in ref. 6 in detail. A schematic diagram of the radial profile of emissivity ($j(\omega)$) is shown in Fig. 4 [5,7]. The frequency f_0 is defined as the non-relativistic 2nd harmonic EC frequency at which the true temperature $T_e^{true}(f_0)$ is equal to the apparent value of the electron temperature $T_e^{obsh}(f_h)$ observed at the given frequency f_h , that is, $T_e^{obsh}(f_h) = T_e^{true}(f_0)$. The frequency shift Δf is defined as $\Delta f = f_0 - f_h$. Related to the shape of emissivity, the frequency shift Δf depends on T_e and n_e , and the B_r structure. Consequently, n_e can be estimated from Δf if the T_e profile and the magnetic structure are known. Fig. 5 shows the comparison between obtained and assumed n_e profile in the case of $T_e(0)=8\text{keV}$. The profile of the electron density $n_e(r)$ is assumed to be power of parabolic function, that is, $n_e(r) = (n_e(0) - n_e(a))(1 - (r/a)^2)^m + n_e(a)$. The power index (m) of parabolic function for n_e profile is changed from 1st to 16th. Obtained $n_e(r)$ in sharp cases is better agreement than that in flat cases, because the locality of T_e in sharp cases is better than that in flat cases.

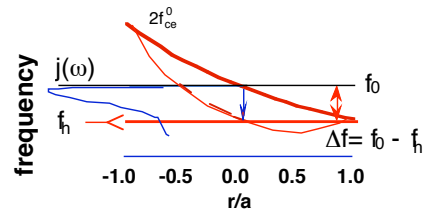


Fig.4 Schematic diagram of radial $j(\omega)$.

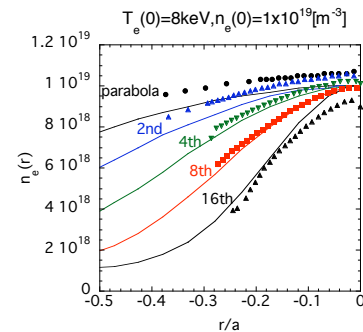


Fig.5. $n_e(r)$ assumed (solid lines) and derived (solid marks).

The work was supported in part by a Grant-in-aid for Scientific Research (C) from the Japan Society for the Promotion of Science.

References

- [1] M. Sato, S. Ishida and N. Isei: J. Phys. Soc. Jpn. **62** (1993) 3106.
- [2] G. Bekefi: *Radiation Processes in Plasmas* (John Wiley and Sons, New York, 1966).
- [3] B. A. Trubnikov: *Magnetic Emission of High-Temperature Plasma, Thesis, Institute of Atomic Energy, Moscow, 1958.*
- [4] M. Sato, A. Isayama, S. Inagaki, Y. Nagayama, et. al: Rev. Sci. Ins. **75** (2004) 3819.
- [5] M. Sato, et. al., *13th Joint Workshop on ECE and ECRH, Nizhny Novgorod, Rusia, 2004.*
- [6] M. Sato, N. Isei, S. Ishida and A. Isayama: J. Phys. Soc. Jpn **67**, 3090 (1998).
- [7] M. Sato, A. Isayama, S. Inagaki, Y. Nagayama et. al: Jpn. J. Appl. Phys. **44** (2005) L672.